Chapter 5

Liquid-liquid Interface as a Viable Platform for the Self-assembly Nanospheres to Nanorods

5. Water/*n*-Heptane Interface as a Viable Platform for the Self-Assembly of ZnO Nanospheres to Nanorods

5.1 Introduction

In recent years, the self-assembly of nanoscale objects has paved the way towards a simple and general strategy to organize nanoparticles into higher order architectures.[1] Such processes require adequate stabilization of the nanoparticles at interfaces with a high degree of organizational selectivity.[1,2] Amongst the three different approaches that are currently exploited to effect ordering of nanoparticles by the self-assembly processes, liquid–liquid interfaces offer an important alternative scaffold for colloidal crystallization into higher ordered nanostructures.[2] A number of innovative approaches have been explored to engender interfacial ordering effects for the organization of nanometer-size objects into both two and three dimensions, including membranes,[3] capsules,[4] core–shell structures,[5] heterodimeric alloyed nanostructures,[6] Janus particles,[7] and giant supramolecular assemblies[8] with distinct functionalities. Nanoobjects made with the semiconductor zinc oxide (ZnO) have attracted immense interest due to its direct wide band gap (3.37 eV), high exciton binding energy (60 meV) and the opportunity to vary its properties by morphological tuning.[9] One-dimensional semiconductor (ZnO) nanostructures (nanowires and nanorods) have attracted special interest due to their fascinating physical properties and potential applications in electronic and photonic devices,[9] room temperature UV laser, dye sensitized solar cell, light emitting diode, varistor, sensor, laser, field emission displays, as high efficient green phosphor, as an UV photodetector materials etc. Due to its present importance and upcoming applications, it is obvious that, tremendous interest has been given to explore various synthetic methods for different particle size, shape and hierarchical assemblies.

Efforts have been made to fabricate one dimensional ZnO nanostructures (nanowires and nanorods) with different ease of synthesis. A variety of synthetic strategies have been adopted in the literature for the fabrication of ZnO nanorods, for example, high temperature physical evaporation,[10] micro-emulsion based hydrothermal process,[11] alcohol thermal process[12] and so on. Yin *et al.*[13] have reported the synthesis of ZnO quantum nanorods by thermal decomposition of zinc acetate (40 mM) in organic solvents in the presence of oleic acid at 286 °C for 1 h under

N_2 flow. Wang and colleague[14] have designed the directed growth of ZnO nanorod arrays on a zinc substrate by the alkaline hydrolysis of zinc foils (15 × 15 × 0.25 mm3) in the presence of Cetyltrimethylammonium bromide loaded into a Teflon-lined stainless steel autoclave by heating at 160 °C for 20 h. Ho and co-authors[15] have developed a solution-based synthesis to grow highly ordered ZnO nanorod-like structures on selective areas of the substrate by heating zinc acetate (5–10 mM) at 90 °C for 8 h in a tightly sealed polypropylene screw cap tube. Guo *et al.*[16] reported the synthesis of ZnO nanorods by ripening the mixture of zinc acetate (50 mM) and potassium hydroxide in methanol at 70 °C, at least, for three days to achieve a narrow size distribution. The Weller group[17] have found that, in a methanolic solution, at a zinc acetate dihydrate concentration of below 10 mM, quasi-spherical particles are formed; whereas mainly nanorods are formed at ten times higher concentration of the precursor. In general, these synthetic methods are carried out with a high concentration of the precursor salt by forced hydrolysis in the presence or absence of a weak base. In this chapter, we have found that the water/n-heptane interface could offer a viable platform for the self-assembly of ZnO nanodots to nanorods using an unconventional low precursor salt concentration (1.0 mM) under facile and benign reaction conditions.

5.2 Experimental

5.2.1 Synthesis of ZnO Nanomaterials

In a typical experiment, an amount of 0.055 g zinc acetate dihydrate was dissolved in 25 mL of solvent mixture (water : *n*-heptane = 9 : 1) in a double-necked round-bottom flask by refluxing in a water bath at 65 °C. After 15 min, 13.5 mL aqueous KOH solution (0.1 mM) was added to the mixture and the refluxing was continued for another 2 h. It was seen that, initially, a faint yellow colouration appeared that slowly transformed to curdy white, indicating progressive transformation of the nuclei into larger particles.[11] Finally, the mixture was cooled to room temperature and stored in the dark.

5.3 Results and Discussion

The progressive transformation of the ultrasmall ZnO particles into larger aggregates has been studied by UV-vis absorption, fluorescence and Fourier transform infrared spectroscopy, X-ray

diffraction and transmission electron microscopy. Figure 5.1 presents the absorption spectra, showing the time evolution of the primarily formed ZnO particles into larger aggregates and the fluorescence spectra of the finally formed particles synthesised at the water/*n*-heptane interface at different time intervals. At the beginning, the absorption spectrum shows two maxima, one at 219 nm (5.66 eV) and the other at 265 nm (4.68 eV), which are characteristic of spherical ZnO nanoparticles. In the case of semiconductor nanoparticles, the Fermi energy level lies in between the valence and conduction band, which is comprised of discrete energy states due to strong electron confinement. These two peaks arise due to the excitonic transitions between the trapped energy states situated within the confinement region.[18]

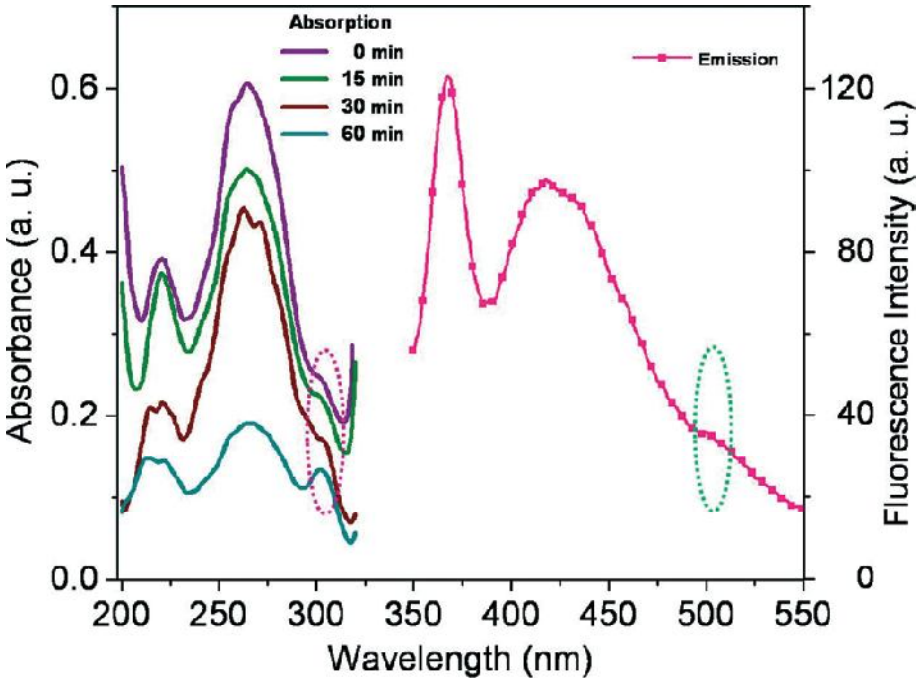

Figure 5.1. Absorbance and fluorescence spectra showing the evolution of ZnO nanospheres to nanorods.

The sizes of the intervening gaps are correlated with the band structure, which again depends on the size of the nanoparticles, on the basis of the interaction with the confined electrons among the lattice points. The optical band edge bears the characteristic electronic transition energy taking place to promote the electrons to the energy states in the conduction band from the valence band, including excitonic effects. As the time progresses, both the peaks decrease in intensity and a new peak at 302 nm (4.11 eV) develops, indicating the gradual transformation of

ZnO nanospheres to nanorods.[16] The fluorescence spectrum (λ_{ex} ~ 302 nm) of the finally formed ZnO particles exhibits a narrow emission band at 379 nm (3.27 eV) that is attributed to the radiative recombination of a hole in the valence band and an electron in the conduction band (excitonic emission).[16] In addition, traces of two emission peaks at ca. 416 nm (2.98 eV) and 434 nm (2.86 eV) are seen that could be attributed to the presence of multiple surface defects in the ZnO nanorods.[19] The absorption and fluorescence spectra, thus, indicate the progressive transformation of the ZnO nanospheres to nanorods.

Figure 5.2 shows the corresponding TEM images of the ZnO particles at the beginning and end of the reaction. It is seen that the initial particles are quasi-spherical in nature with average particle sizes of 3–5 nm, while the rod-shaped particles are ca. 100–200 nm and 15–20 nm in length and diameter, respectively. The corresponding selected area electron diffraction patterns (shown in the inset) reveal the appearance of polycrystalline-like diffraction, which is

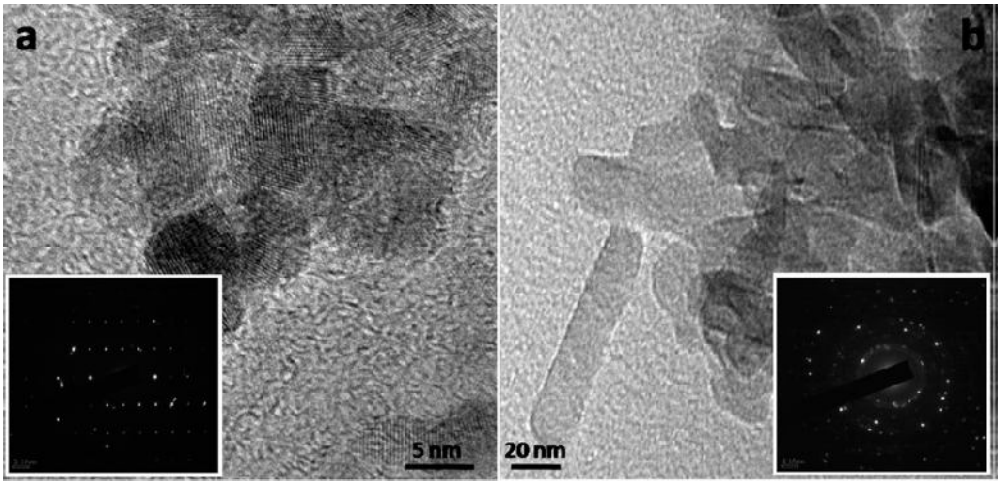

Figure 5.2. Representative TEM images of ZnO particles at the (a) beginning and (b) end of the reaction. Insets show the corresponding selected area electron diffraction patterns of the ZnO nanostructures.

consistent with reflections (100), (002), (101), (102) and (110), corresponding to the hexagonal wurtzite phase of ZnO particles, indicating that the nanorod is an ordered assembly of small nanocrystals sub-units without crystallographic orientation.[20] Detailed TEM investigations during the formation of the nanorods are presented in Figure 5.3. At low magnification, aggregated quasi-spherical particles are seen (panel a) and these subsequently form pearl-chain-like structures (panel b). It could be recognized that the particles are epitaxially fused together,

and bottlenecks between the adjacent attachments are seen along the c-axis (002), but laterally oriented attachment parallel to the c-axis is also evident (panel c). In some cases, it is apparent that the individual particles are aligned like a wall, where the second layer of bricks is just starting to be put on the particles that are still visible. Therefore, it is evident that the nanorods are formed by coalescence through the 'oriented attachment' of quasi-spherical particles. This

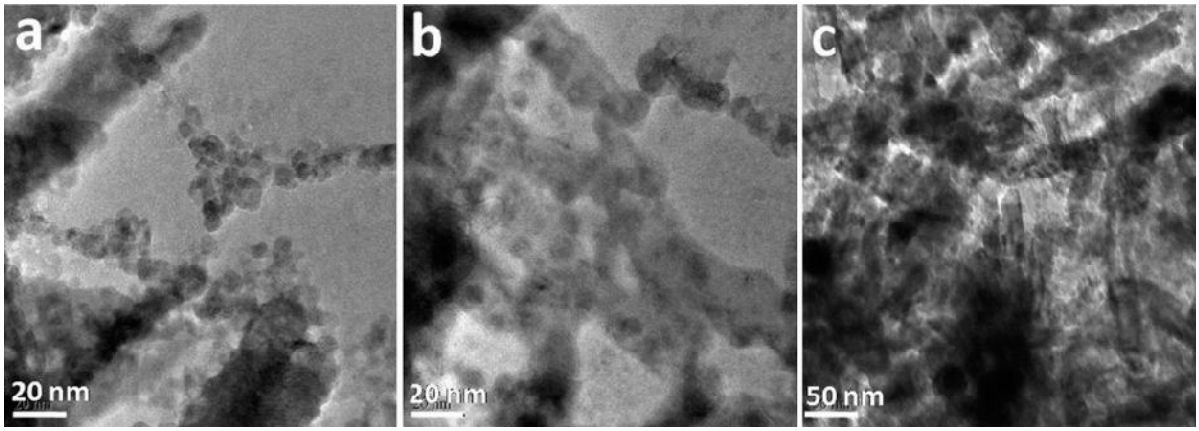

Figure 5.3. TEM investigations during the formation of nanorods (a) 15, (b) 30 and (c) 45 min of reflux.

model of transformation of ZnO nanospheres to nanorods has been evidenced by the Weller group.[17] Oriented attachment has, previously, been proposed by other authors during the crystal growth of iron oxide, TiO_2 with sizes of a few nm and for micrometer sized ZnO particles during the formation of rod-like ZnO microcystals.[21–23]

Figure 5.4 shows the high resolution TEM images of single ZnO nanorods with various magnifications. It is seen that the lattice planes of the depicted nanorods are almost perfectly aligned, with a lattice fringe of 0.26 nm consistent with the d_{002} spacing of wurtzite ZnO

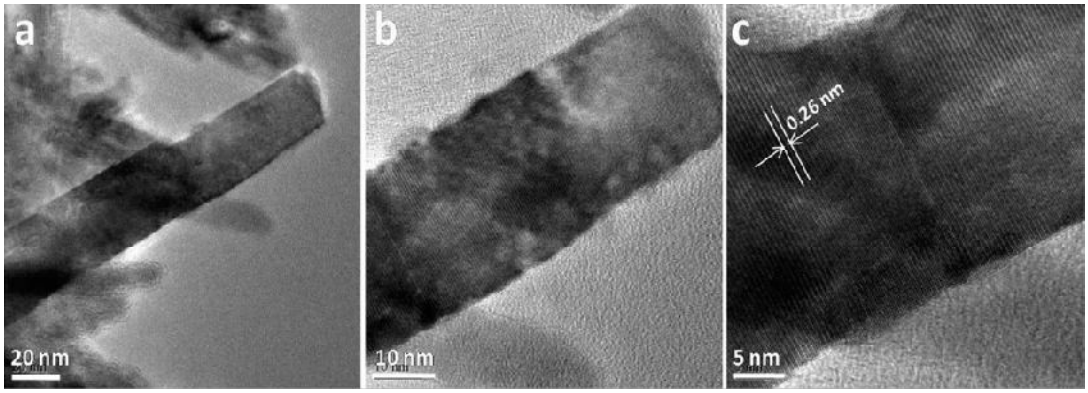

Figure 5.4. TEM images of ZnO nanorods with increasing magnifications.

nanostructures.[24] Moreover, it could be recognized that the lattice planes go straight through the contact areas of the small spherical nanocrystals. Figure 5.5 shows the FTIR spectra of growing ZnO nanostructures at different time intervals. With increasing reflux time, it is seen that a peak at ca. 458 cm^{-1}, assigned to the stretching vibration of Zn–O bonds, is sharpening with time,

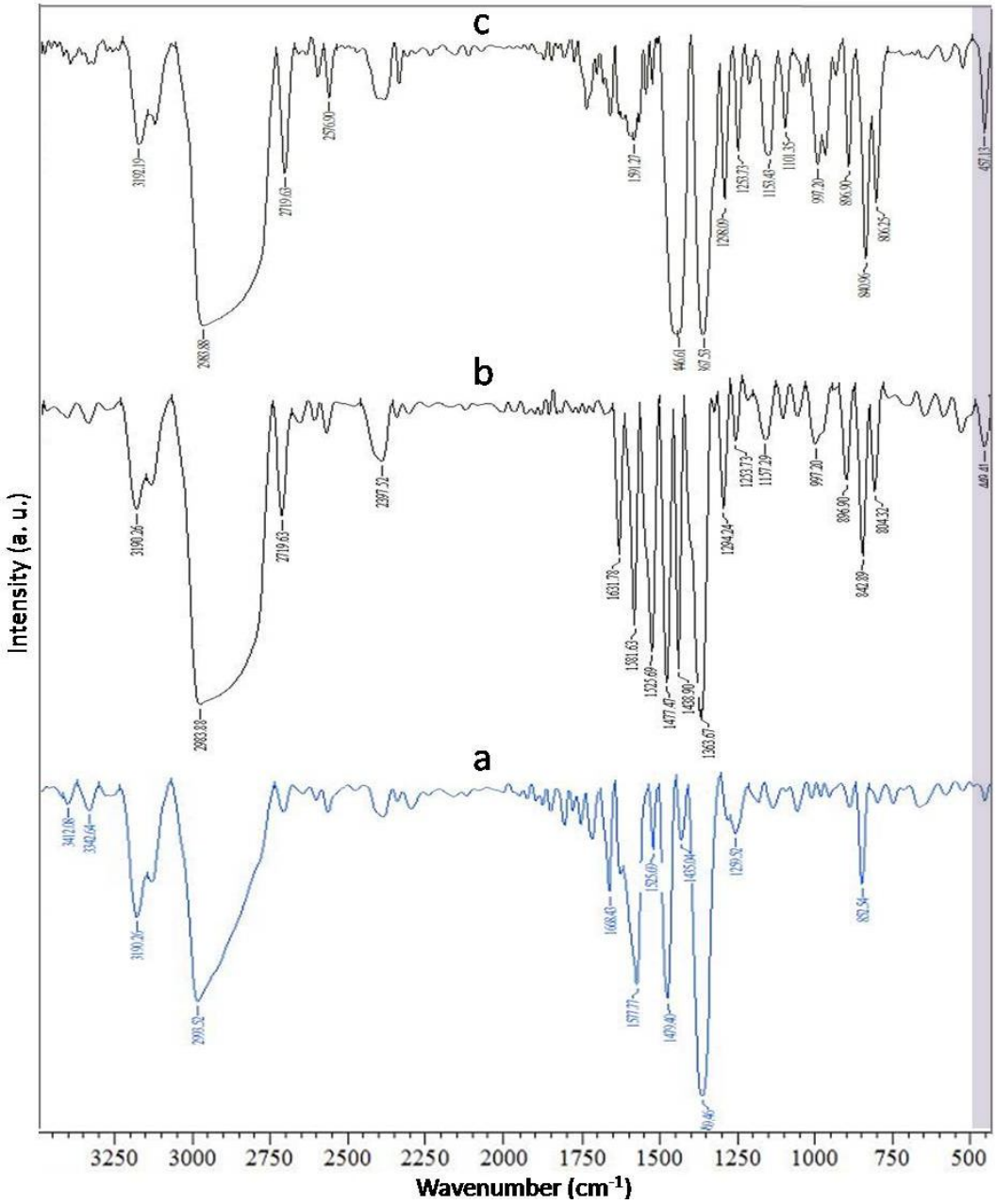

Figure 5.5. FTIR spectra taken during the transformation of ZnO nanospheres to nanorods after (a) 0, (b) 30 and (c) 90 min of refluxing. The shaded area indicates the area of interest.

indicating the crystallization of ZnO into higher order architectures.[23] Moreover, other peaks at *ca.* 805, 853 and 863 cm^{-1} exhibit similar trends with increasing reflux time.[25] In addition, strong absorption at 3442 cm^{-1} and weak absorptions around the 2800 to 3000 cm^{-1} region reveal the stretching vibrations of O–H and C–H, respectively. The absorption peak at 1104 cm^{-1} corresponds to the C–OH stretching and O–H bending vibrations, whereas the bands at 1383, 1577, and 1630 cm^{-1} correspond to C–O (hydroxyl, ester, or ether) stretching and O–H bending vibrations.[26] Therefore, it could be conceived that the dominant growth mechanism of ZnO nanorods is mainly the oriented attachment mechanism. The concomitant appearance of other bands indicates the presence of organic residues on the surface of the nanospheres that remain even after the formation of nanorods.

X-ray diffractograms of as-prepared ZnO samples with various reflux times are shown in Figure 5. 6. All patterns could be indexed to the pure hexagonal phase of Zn with a space group of C_{6v}^{4} and cell constants a = 3.25 Å, and c = 5.21 Å (JCPDS card no.: 76-0704), which suggests that the product comprises ZnO nanocrystals with the wurtzite structure.[27] An increase in refluxing time increases the relative intensities of the (002) diffraction line, which is consistent with the rod formation along the c-axis of the particles.[24]

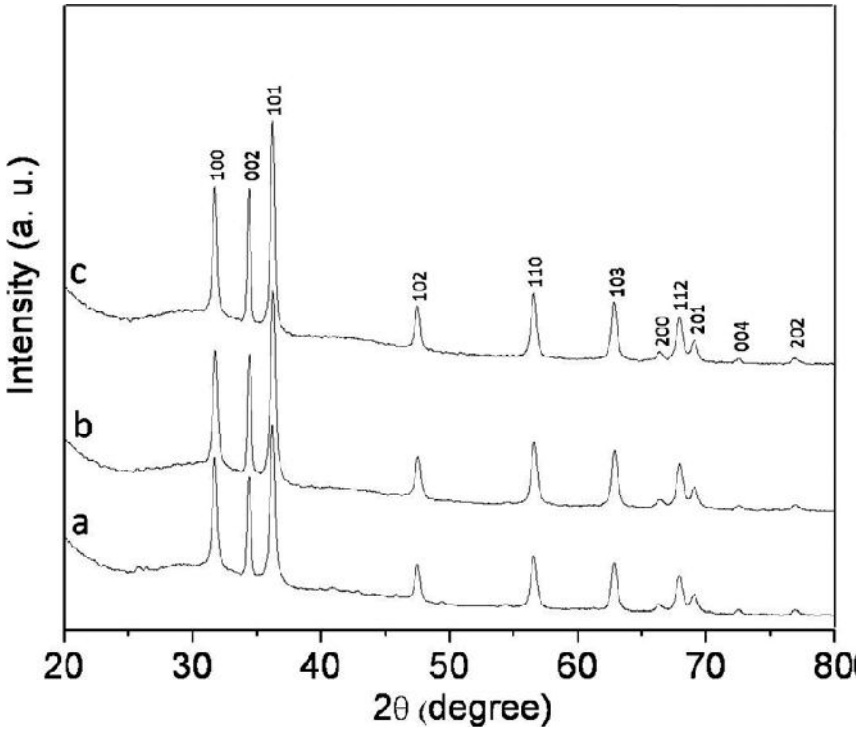

Figure 5.6. X-ray diffractograms of the transformation of ZnO nanospheres to nanorods (a) 30 min (b) 1 h and (c) 2 h of reflux.

To elucidate the mechanism of transformation of ZnO nanospheres to nanorods at the liquid–liquid interface, a series of experiments was carried out. It is noted that the transformation to nanorods does not occur at the prescribed low precursor concentration in the presence of polar solvents, consistent with earlier observations.[17] The formation of the nanorods was tried in the presence of six water-immiscible solvents viz. cyclohexane, n-heptane, benzene, toluene, o-xylene and dichloromethane, and the fluorescence spectra (λ_{ex} ~ 302 nm) of the finally formed particles were measured (Figure 5.7). The appearance of a new band at 503 nm only in the presence of *n*-heptane made us curious about the uniqueness of the morphology of the particles formed at the water/*n*-heptane interface.

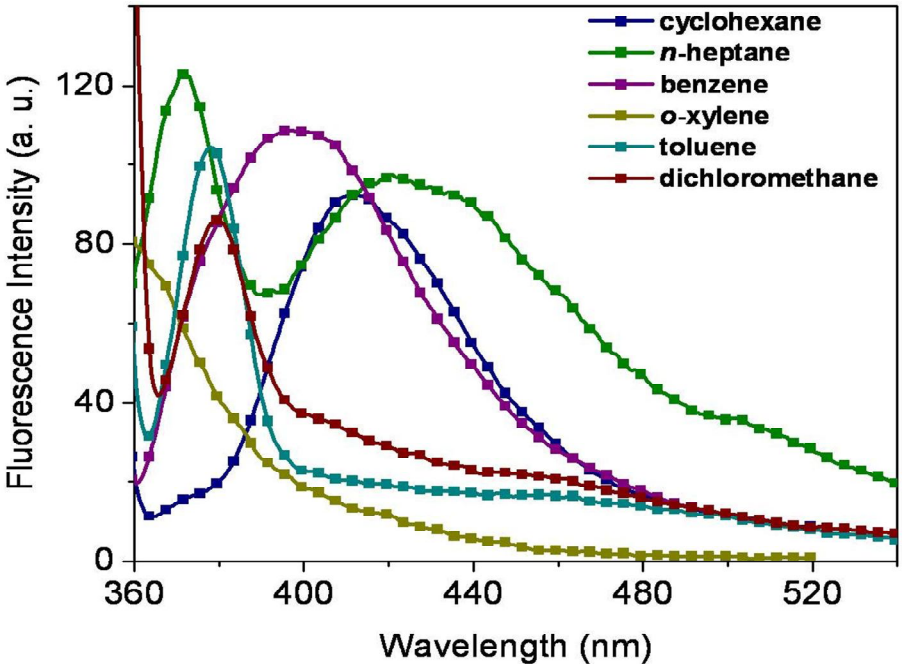

Figure 5.7. Emission spectra of the finally formed ZnO nanostructures at the aqueous/organic liquid pairs

The TEM images of the particles formed in the presence of two other representative solvents, *viz.*, dichloromethane and cyclohexane, are shown (Figure 5.8). The transformation of the quasi-spherical particles to rods was not seen in any of these solvents. It is now well-established in the literature that the formation of the nanorods requires anisotropic crystal growth, based on the surface and attachment energies of various crystallographic planes,[17,21–23] When the present experiment is carried out in the absence of organic solvent, keeping all other experimental

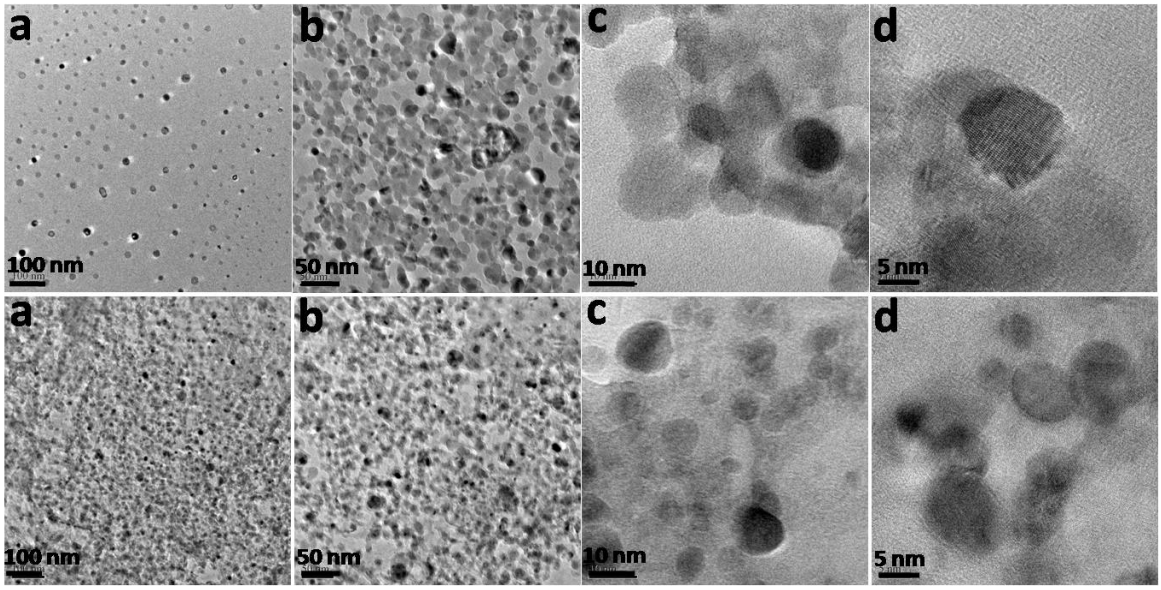

Figure 5.8. TEM images with increasing magnification of the formation of particles at (top) water/dichloromethane and (bottom) water/cyclohexane interface.

conditions unaltered, there is formation of ultrasmall ZnO nanoparticles. Therefore, it could be conceived that water/ *n*-heptane interfacial tension offers the requisite restricted environment for

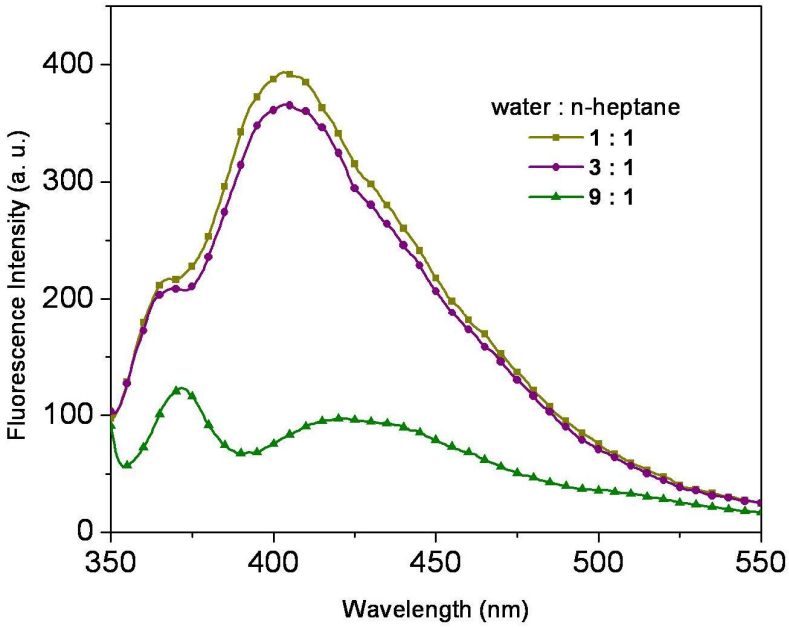

Figure 5.9. Fluorescence spectra of the finally formed ZnO nanostructures at different water/*n*-heptane volume ratio.

the oriented attachment of the nanospheres to form nanorods. The composition of the solvent also plays a role for the transformation of nanospheres to nanorods. The fluorescence spectra obtained by varying the water/*n*-heptane composition are shown in Figure 5.9. It is seen that a new band appears at 503 nm only in the presence of *n*-heptane at a volume ratio of water : *n*-heptane = 9 : 1; at a volume ratio above or below, the appearance of no such band is observed. Therefore, it could be concluded that formation of the nanorods is favored at an optimum composition of the water and *n*-heptane mixture. It is now well established in the literature that a liquid–liquid interface is a non-homogeneous region, having a thickness of the order of a few nanometers.[28] The interface between two immiscible liquids, thus, offers an important scaffold for the chemical manipulation and self-assembly of the nanocrystals.[29] The interfacial tension at the water/n-heptane interface is dependent upon solvent composition. Therefore, it is manifested that, while the liquid–liquid interface offers a viable platform, the observed assembly is the result of specific interparticle interactions bringing about the transformation to nanorods. The attachment does not occur at room temperature, pointing out that a moderately higher temperature (65 °C; below the boiling point of *n*-heptane, 98.42 °C) helps to tailor the fusion of the particles. When two ZnO building blocks come together, the capillary forces between them facilitate the solvent removal and strengthen the agglomerate by van der Waals' forces. Finally, with an increase in reaction time, directed self-assembly of the oriented nanocrystallites and subsequent fusion lead to the formation of ZnO one dimensional nanorods [30] Therefore, on the basis of the above experimental results, a plausible mechanism for the transformation of ZnO nanospheres to nanorods through the oriented attachment of the ultrasmall particles could be developed, as depicted in Scheme 5.1.

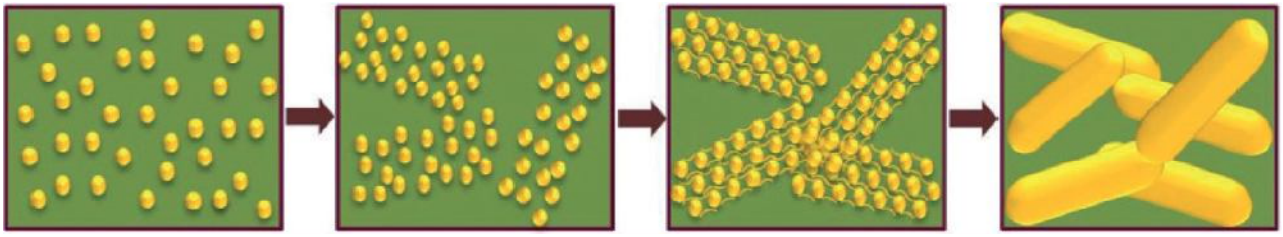

Scheme 5.1. Schematic presentation of the formation of nanorods from nanospheres.

5.4 Conclusions

A liquid–liquid interface has been exploited as a viable platform for the oriented attachment of quasi-spherical ZnO nanoparticles to form single crystalline nanorods under the prescribed reaction conditions. The formation of ZnO nanorods could be achieved at a very low concentration of the precursor in a restricted environment created by a particular composition of polar/non-polar liquid pairs. Incidentally, the transformation occurs selectively at the water/n-heptane interface, offering production of the nanorods under environmentally benign conditions.

5.5 References

(1) Katz, E.; Shipway, A. N.; Willner, I. In *Nanoscale Materials*, ed. Liz-Marzan, L. M. and Kamat, V. P. eds. Kluwer Norwell, **2003**, pp. 317–343.

(2) Binder, W. H. *Angew. Chem. Int. Ed.* **2005**, *44*, 5172-5175.

(3) Lin, Y.; Skaff, H.; Böker, A.; Dinsmore, A. D.; Emrick, T.; Russell, T. P. *J. Am. Chem. Soc.* **2003**, *125*, 12690-12691.

(4) Duan, H.; Wang, D.; Kurth, D. G.; Möhwald, H. *Angew. Chem. Int. Ed.* **2004**, *43*, 5639-5642.

(5) Niu, Z.; He, J.; Russel, T. P.; Wang, Q. *Angew. Chem. Int. Ed.* **2010**, *49*, 10052-10066.

(6) Gu, H.; Yang, Z.; Gao, J.; Chang, C. K.; Xu, B. *J. Am. Chem. Soc.* **2005**, *127*, 34-35.

(7) Gröschel, A. H.; Walther, A. L; Obling, T. I.; Schmelz, J.; Hanisch, A.; Schmalz, H.; Müller, A. H. E. *J. Am. Chem. Soc.* **2012**, *134*, 13850–13860.

(8) Ali, M.; Pal, S. K.; Rahaman , H.; Ghosh, S. K. *Soft Matter* **2014**, *10*, 2767–2774.

(9) Wang, Z. L. *Appl. Phys. A: Mater. Sci. Process.*, **2007**, *88*, 7–15.

(10) Wang, Y. W.; Zhang, L. D.; Wang, D. J.; Peng, X. S.; Chu, Z. Q.; Liang, C. H. *J. Cryst. Growth* **2002**, *234*, 171–175.

(11) Zhang, J.; Sun, L. D. H.; Pan, Y.; Liao, C. S.; Yan, C. H. *New J. Chem*. **2002**, *26*, 33–34.

(12) Cheng, J. B.; Zhang, X. B.; Tao, X. Y.; Lu, H. M.; Luo, Z. Q.; Liu, F. *J. Phys. Chem. B* **2006**, *110*, 10348–10353.

(13) Yin, M.; Gu, Y.; Kuskovsky, I. L.; Andelman, T.; Zhu, Y.; Neumark, G. F.; O'Brien, S.; *J. Am. Chem. Soc*. **2004**, *126*, 6206–6207.

(14) Wang, D.; Song, C. *J. Phys. Chem. B* **2005**, *109*, 12697–12700.

(15) Wang, C. H.; Wong, A. S. W.; Ho, G. W. *Langmuir* **2007**, *23*, 11960–11963.

(16) Guo, Y.; Cao X.; Lan, X.; Zhao, C.; Xue, X.; Song, Y. *J. Phys. Chem. C* **2008**, *112*, 8832–8838.

(17) Pacholski, C.; Kornowski, A.; Weller, H. *Angew. Chem., Int. Ed*. **2002**, *41*, 1188–1191.

(18) Alivisatos, A. P. *Science* **1996**, *271*, 933–937.

(19) Kahn, M. L.; Cardinal, T.; Bousquet, B.; Monge, M.; Jubera, V.; Chaudret, B. *ChemPhysChem* **2006**, *7*, 2392–2397.

(20) Ge, M. Y.; Wu, H. P.; Niu, L.; Liu, J. F.; Chen, S. Y.; Shen, P. Y.; Zeng, Y. W.; Wang, Y. W.; Zhang, G. Q.; Jiang, J. Z. *J. Cryst. Growth* **2007**, *305*, 162–166.

(21) Banfield, J. F.; Welch, S. A.; Zhang, H.; Ebert, T. T.; Penn, R. L. *Science*, **2000**, *289*, 751–754.

(22) Chemseddine, A.; Moritz, T. *Eur. J. Inorg. Chem.* **1999**, 235–245.

(23) Andres Verges, M.; Mifsud, A.; Serena, C. J. *Faraday Trans.*, **1990**, *86*, 959–963.

(24) Krishnan, D.; Pradeep, T. *J. Cryst. Growth* **2009**, *311*, 3889–3897.

(25) Joshi, K. M.; Shrivastava, V. S. *Appl. Nanosci.*, **2011**, *1*, 147–155.

(26) Sevilla, M.; Fuertes, A. B. *Chem. Eur. J.* **2009**, *15*, 4195–4203.

(27) Goano, M.; Bertazzi, F.; Penna, M.; Bellotti, E. *J. Appl. Phys.*, **2007**, *102*, 083709–083719.

(28) Böker, A.; He, J.; Emrick, T.; Russell, T. P. *Soft Mat.* **2007**, *3*, 1231-1248.

(29) Nykypanchuk, D.; Maye, M. M.; van der Lelie, D.; Gang, O. *Nature* **2008**, *451*, 549-552.

(30) Fernández-Garcia, M.; Rodriguez, J. A. In *Nanomaterials: Inorganic and Bioinorganic Perspectives* Lukehart, C. M.; Scott, R. A. eds. John Wiley & Sons, West Sussex, UK, **2008**, p. 453.